

# Stray field ring resonators and a novel trough guide resonator for precise microwave moisture and density measurements

Reinhard Knöchel<sup>1</sup>, Wolfgang Taute<sup>1</sup> and Claas Döscher<sup>2</sup>

<sup>1</sup> Lehrstuhl für Hochfrequenztechnik, Technische Fakultät, Universität Kiel, Kaiserstrasse 2, 24143 Kiel, Germany

<sup>2</sup> Döscher&Döscher Ingenieurbüro GmbH, Grandweg 63, 22529 Hamburg, Germany

E-mail: [rk@tf.uni-kiel.de](mailto:rk@tf.uni-kiel.de) and [info@doescher.com](mailto:info@doescher.com)

Received 26 April 2006, in final form 9 July 2006

Published 27 February 2007

Online at [stacks.iop.org/MST/18/1061](http://stacks.iop.org/MST/18/1061)

## Abstract

The paper first describes the design and construction of two different kinds of quasi-planar stray field ring resonators for microwave moisture and density measurements, which are typical for the state of the art, and then the practical performance of such sensors. The changes in resonant frequency and resonator bandwidth are utilized for the determination of the moisture content or the material's density. Nonlinear temperature behaviour is identified as a critical property of conventional stray field resonators, which restricts their measurement accuracy. A novel trough guide resonator is then presented which is entirely manufactured from a ring of alumina oxide ceramics and overcomes the temperature problems. The ring is metallized at its surface except at the front face, which permits a stray field to come into contact with the material under test. The described resonator is capable of withstanding considerable abrasive forces without having a protective cover. At the same time it shows excellent linear and predictive temperature behaviour, which allows precise compensation of the inherent temperature dependence of the resonator. Under constant environmental conditions, the sensibility and accuracy of the old and new resonator designs are exactly the same. However, at varying temperature, an error can be removed to a much higher extent for the new resonators, restricting deviations in the moisture content caused by temperature to typically less than 0.1%, as compared to errors of up to several per cent for the previous designs over a temperature range of ~20–50 °C.

**Keywords:** moisture measurement, density measurement, microwave resonator, stray field

(Some figures in this article are in colour only in the electronic version)

## 1. Introduction

Microwave resonators can be utilized for accurate online monitoring of the moisture content and the mass or the density of materials in production processes. The materials under test are often bulk solids. Online moisture measurements are required, e.g., for regulating dryers, for conditioning materials

or for maintaining the quality of a product, whereas mass or density measurements have to be carried out, e.g., for dosage of ingredients or for packing products in certain quantities. In this paper, moisture content, on a wet basis, is expressed as

$$\Psi = \frac{m_w}{m_w + m_d}, \quad (1)$$

where  $m_w$  is the mass of water and  $m_d$  is the mass of dry matter in the measurement volume  $V$ . Loading the electrical field of a resonator with a moist material results in a decrease in the resonant frequency due to an increase in stored electrical energy and a widening of the bandwidth due to increased dissipation losses in comparison to the empty resonator, which serves as a reference. Both the resonant frequency decrease  $\Delta f$  and the bandwidth increase  $\Delta B$  depend on the moisture content  $\Psi$  and the total mass  $m_{\text{tot}} = m_w + m_d$  of the material sample or the density  $\rho = \frac{m_{\text{tot}}}{V}$  in the fields of the resonator. Careful examination shows, however, that the ratio of both quantities is virtually independent of the mass and thus only a function of the moisture content (Meyer and Schilz 1980):

$$\frac{\Delta B(\Psi, m_{\text{tot}})}{\Delta f(\Psi, m_{\text{tot}})} = M(\Psi). \quad (2)$$

$M(\Psi)$  may be called a ‘moisture function’. It is largely dependent on the measured material. After the moisture content  $\Psi$  is determined from equation (2), the mass can be found from, e.g., the resonant frequency decrease  $\Delta f$ . Hence the moisture content and mass can be determined independently, and either a mass- (density-) independent moisture measurement or a moisture-independent mass measurement can be carried out. Such two-parameter measurements are only possible within certain ranges of moisture content and density in the measurement volume. A given material must be tested whether the sketched approach works for it or not. Certain materials exist which cannot be tested in that way, for reasons which are not always entirely clear. However, the approach works excellent and is highly accurate at moderate moisture levels (i.e. typically 0.5–1% to 20–25%) for a wide range of natural materials such as wool, tobacco, ground coffee or wood chips, just to mention some examples.

The resonator, which is used as a sensor, has to be tailored to fit into the production line. One solution is to use a resonant cavity with a channel where the material can be guided through. If this is inconvenient, open resonant structures may be employed, which can be flush mounted onto a surface and evolve an associated stray field. The material to be analysed is guided along the surface through the stray field, thus producing the measurement effect. The versatility of the stray field resonators makes them particularly interesting and important for practical applications. This paper deals with the construction of several specific, yet typical, designs of such stray field resonators and with problems which may occur during their practical application at varying temperature. A new type of stray field resonator will be presented, which shows a rugged design and excellent performance with respect to measurement accuracy over a wide temperature range.

## 2. Stray field resonators

Stray field resonators are open structures and thus prone to radiation of electromagnetic energy. For the described application possible radiation losses have to be avoided or at least have to be negligible in comparison to losses in the measured material. This has to be guaranteed by the construction. Radiation losses would lead to a widening of the resonator bandwidth which could not be distinguished from

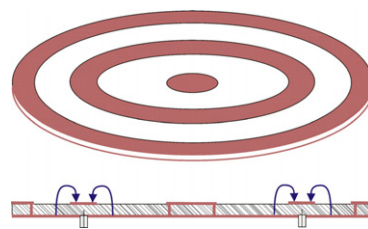


**Figure 1.** Microstrip ring resonator. The ring in the middle forms the resonator. The inner and outer top metallization is connected to the ground by via holes for shielding purposes. Two connectors serve for coupling of the resonator.

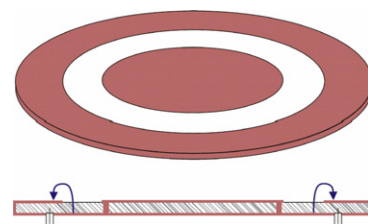


**Figure 2.** ‘Rectangular-waveguide’ ring. The inner top metallization is connected to the ground by via holes. The outer metallization forms a kind of rectangular-waveguide ring, where part of the top metallization is removed.

that caused by absorption in the material, leading to errors in the moisture and density measurements. Ring resonators are very well suited for the desired purpose. They have been widely used at microwave frequencies for the determination of effective permittivities of transmission lines. For ring resonators no open- or short-circuited line ends are present, which could cause radiation. Another important step for the avoidance of radiation is to ensure that the wavelength on the ring at resonance is much shorter than the free wavelength in the material. This requirement can be met if the ring resonator is constructed from a material having a permittivity much higher than the effective permittivity of the moist material.

### 2.1. Conventional ring resonators

Examples of resonator constructions are given in figures 1 and 2. Figure 1 shows a microstrip ring as first proposed for moisture measurements by Flemming and Plested (1988). The resonator of figure 2 can be interpreted as a ring of rectangular waveguide, whose cross section can be seen in the lower part of the picture. Part of the top metallization is removed at the inner half in order to allow the stray field to enter the test material on top. The central metal patch is grounded by a close fence of metallized via holes at its outer edge. Other shapes of resonators have been proposed, such as a dielectrically filled flat plate  $E_{\text{np0}}$  resonator, which has a central hole in its top plate (Herrmann and Zaage 2001). The circumference of the ring resonators is typically 6–8 wavelengths. They are typically manufactured from cheap ceramic-filled plastic substrates with copper cladding. The resonant structures are defined by etching. A widely used material is TMM10 from Rogers Corporation (2002). TMM10 has a dielectric constant of 9.2 and a loss tangent of 0.0023. It consists of a hydrocarbon thermoset ceramic-filled plastic material with inherent temperature compensation.

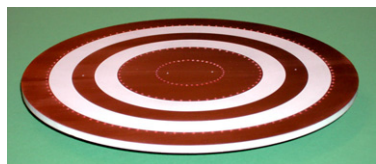


**Figure 3.** Microstrip ring resonator at 2–3 GHz, manufactured from TMM10<sup>®</sup>. The resonant ring has a diameter of approximately 12 cm.



**Figure 4.** 'Rectangular-waveguide' resonator at 2–3 GHz, manufactured from TMM10<sup>®</sup>.

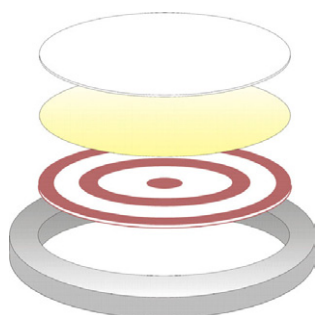


**Figure 5.** Exploded view of the microstrip resonator in its fixture. An alumina plate (on top) is glued (second layer) onto the etched pattern (third layer). The whole assembly is then bedded into a support of, e.g., stainless steel, which fits flat into a surface carrying the material.

The temperature coefficient of the dielectric constant is  $-38 \text{ ppm } ^\circ\text{C}^{-1}$ . Copper is directly clad onto the surface. Two manufactured resonators are depicted in figures 3 and 4.

The resonators as shown are not directly usable in practice. They have to be placed into a final assembly as displayed in figure 5. For protection of the etched copper cladding against abrasive forces caused by the material under test, a hard ceramic layer has to be fixed onto the etched pattern. This will prevent the immediate destruction of the metallization. Typically, the cover is a plate of alumina ( $\text{Al}_2\text{O}_3$ ) with a thickness of  $\sim 0.2 \text{ mm}$ . Alumina has a dielectric constant of 9.8 and is thus well matched to TMM10. The plate has to be glued to the resonator. Epoxy can be used for that purpose. However, the dielectric constant of epoxy is approximately 4, and thus a thin gap filled with low permittivity material appears between the two other layers. The electric field lines cross this gap approximately at right angles and a comparatively high electrical field strength is developed in the glue layer. It thus has quite a high influence on the total frequency behaviour. Another aspect is that the glue has to provide a holohedral bond which is sometimes difficult to achieve, hampering the reproducibility of the whole assembly. If the resonators are built up as described, an effective permittivity as seen by the standing wave in the microstrip ring resonator

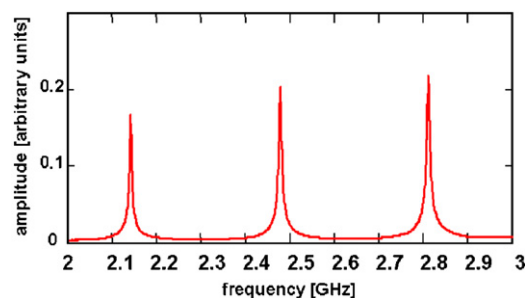


**Figure 6.** Measured resonant frequency spectrum of the microstrip ring resonator. Three resonances appear in the frequency range between 2 and 3 GHz, which can be equally used for measurement purposes.

of approximately 7.5 appears. If the resonator is used for monitoring materials with not too high densities and moisture contents, such as, e.g., wood particles, which may have an effective permittivity of less than 4.5, the radiation of the microwave into the material is sufficiently suppressed in order to carry out accurate measurements. The described structures are used as transmission resonators. Input and output couplings are situated at opposite locations on the rings although other places are also possible. The transmission scattering coefficient  $s_{21}$  is monitored for moisture and density determination of the material under test. The measured resonant frequency spectrum of a microstrip ring resonator is shown in figure 6. There are three resonances in the frequency range between 2 and 3 GHz, which is the intended operating range of the resonator. However, for this type of resonator the resonances start to appear at approximately 300 MHz and extend well beyond 5 GHz. They could be utilized over the whole range of frequencies. The resonance spectrum of the 'rectangular-waveguide resonator' (figure 4) starts at approximately 1.3 GHz, which is defined by the cut-off frequency of the chosen waveguide. Above approximately 3 GHz the resonance spectrum is distorted for this resonator, because the waveguide becomes overmoded. Within 2–3 GHz, however, the mode spectrum looks as clear as that of the microstrip resonator, and both resonators can be used with quite similar performance.

## 2.2. Temperature behaviour

Resonators for online monitoring of materials are often used over wide temperature ranges. An example is the application of a moisture meter for the regulation of a dryer. In such a case, the material under test will be at a high and varying temperature and will also heat up the resonator. Temperature sensors are employed which will determine the temperature of the material under test and of the resonator as well. Typical behaviour of the resonance curve at increasing temperature is illustrated schematically in figure 7. Due to heating, the resonator will thermally expand and thus its resonant frequency will be lowered. Simultaneously, the temperature coefficient of the dielectric material of the resonator will also contribute to resonant frequency changes. In total, the resonant frequency  $f_0$  will be lowered as compared to the empty resonator (in air), which is taken as the reference, as was stated earlier. Temperature, however, does not only affect the resonant

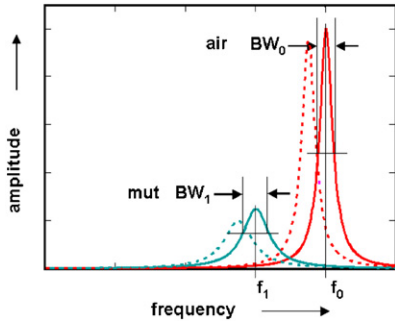


**Figure 7.** Temperature characteristics of a resonator. The solid lines denote the resonance curves for the empty resonator (air) and loaded with a material under test (mut) at the reference temperature  $T_0$ , whereas the broken lines describe the respective resonances at a temperature  $T_{high}$ . In air the resonator has the resonant frequency  $f_0$  and the bandwidth  $BW_0$ . Loaded with a material under test (mut) this changes to  $f_1$  and  $BW_1$ .

frequency but also bandwidth. This mainly takes place because the losses due to limited conductivity of metallization and due to limited skin depth as well as losses in the substrate material also vary. Hence, the bandwidth  $BW_0$  of the empty resonator will slightly increase at rising temperature. In principle, the coupling of the resonator to the measurement electronics will also change. However, with the described resonators, this has only a minor influence, because weak (undercritical) coupling is used. New reference values for the empty resonator must be deduced from the original values under online operation. Since a new empty measurement cannot be regularly carried out, a model for temperature behaviour of the resonator has to be assumed and the new reference values are determined through calculation. Under practical conditions, only linear temperature dependence can be taken into consideration and will work reliably. A nonlinear model would require too much calibration effort.

Errors in the reference values would directly translate into errors for the moisture content or the density (mass) measurement. To this end equation (2) is analysed concerning the influence of errors in the bandwidth and frequency determination, denoted by  $d\Delta B$  and  $d\Delta f$

$$\frac{d\Psi}{\Psi} = \frac{1}{\Psi} \frac{dM}{M} \left[ \frac{d\Delta B}{\Delta B} - \frac{d\Delta f}{\Delta f} \right]. \quad (3)$$

The error depends on the slope of the moisture function  $M$ . A typical characteristic of the moisture function is sketched in figure 8(a). Similar characteristics were empirically determined for numerous tested materials. At very low moisture values the behaviour is approximately quadratic. Then it becomes linear and gradually flattens until the maximum measurable moisture value is approached. The factor before the brackets in equation (3) is depicted in figure 8(b). It can be deduced that the relative error in the moisture measurement is proportional to the relative errors in bandwidth and resonant frequency measurement, but this error will be boosted by the nonlinearity of the moisture function the more the actual moisture content approaches the maximum measurable moisture value.

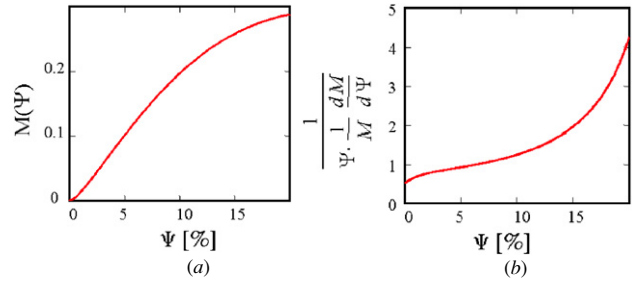


**Figure 8.** (a) Typical characteristics of the moisture function  $M(\Psi)$ . At very low moisture content the behaviour is approximately quadratic. It then becomes increasingly linear and gradually flattens until the maximum measurable moisture content is reached, which is often around  $\sim 25\%$ . (b) A factor describing the dependence of the error in the relative moisture value on the measurement errors in relative bandwidth and resonant frequency.

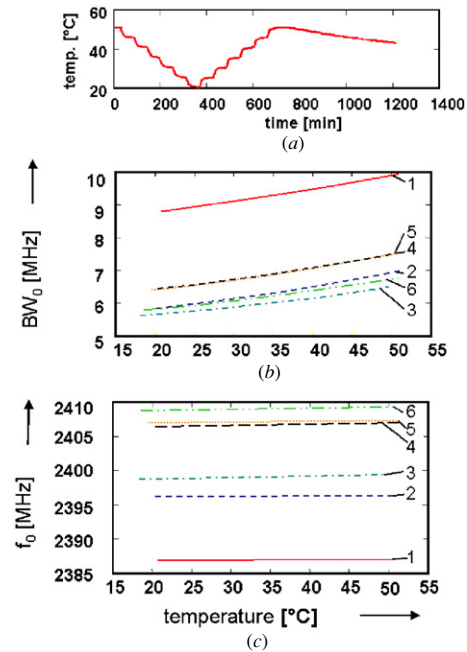


**Figure 9.** Temperature cycling of six different microstrip resonators. (a) The resonators were heated up to approximately  $52^\circ\text{C}$ , then cooled down to around  $20^\circ\text{C}$  in  $5^\circ\text{C}$  steps and heated up again. Then the heating was switched off. (b) Temperature behaviour of bandwidth and (c) of resonant frequency. The numbers correspond to the respective resonators.

### 2.3. Temperature characteristics of the microstrip ring resonator

Six manufactured microstrip ring resonators as shown in figure 3 and assembled as described in figure 5 were temperature cycled in a temperature exposure cabinet. The applied temperature pattern is shown in figure 9(a). After heating up to approximately  $50^\circ\text{C}$  the resonators were slowly cooled down to around  $20^\circ\text{C}$  in steps of  $5^\circ\text{C}$ , then heated up again and finally left alone after switching off the heating. A temperature step was retained long enough to ensure homogeneous heating of the whole assembly. At the end of the heating cycle, the concluding cooling process was slow enough to maintain thermal equilibrium. Figures 9(b) and



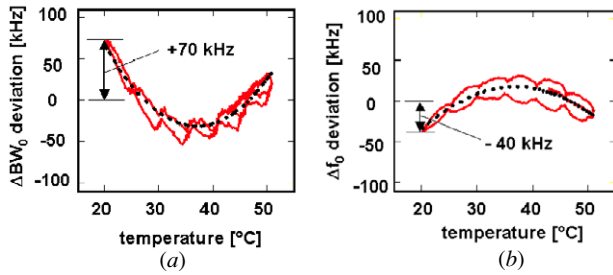


**Figure 10.** Frequency deviation from a linear behaviour of (a) bandwidth and (b) resonant frequency versus temperature. The solid curves indicate the characteristics of one of the resonators, whereas the broken curves denote the average of the six investigated resonators.

(c) show the associated changes of bandwidth and resonant frequency of the empty resonators with temperature. The resonant frequencies and bandwidths of the various resonators are somewhat different due to manufacturing and coupling tolerances. It can be observed that the resonant frequencies are quite stable over the temperature range. This is due to the inherent temperature compensation of TMM10.

As a next step, straight lines were fitted to the temperature curves of bandwidths and resonant frequencies, which had the lowest deviations from the measured curves. The linear changes were subtracted and the deviations were recorded. The solid curves in figures 10(a) and (b) denote the result for one of the six resonators. The dotted curves display the averages for six resonators. The solid curves show a distinct nonlinearity for both the bandwidth and the resonant frequency of the assembled microstrip resonator. When up-cycling and down-cycling the temperature, frequency deviations occur, which are due to a dynamic process and inhomogeneous heating. The points of closest approximation of the upper and lower curve branches indicate where at every 5 °C step the temperature was kept constant and thermal equilibrium was allowed to appear. Especially in the resonant frequency deviation, it is obvious that a certain hysteresis occurs. This is due to the materials involved and the stratified construction

with the protective alumina cover on top, the glue and the resonator itself.

It can be read from figure 10 that the maximum bandwidth deviation at about 20 °C is approximately  $d\Delta B = 70$  kHz, which occurs together with a deviation in the resonant frequency of  $d\Delta f = -40$  kHz. Both errors would adulterate the reference values in moisture measurements and give rise to a measurement error in the moisture content. If tobacco is taken as an example, one comes upon the following typical values: a moisture content of  $\Psi = 10\%$  at a certain material density causes, e.g., a bandwidth increase of  $\Delta B = 500$  kHz and a frequency shift of  $\Delta f = 2500$  kHz. Application of equation (3) suggests that due to resonator temperature deviation a measurement error for the moisture content of approximately  $\Delta\Psi = 1.5\%$  may occur.

The described temperature effect illustrates an obvious flaw of resonator construction, which is based on surface definition of etched or otherwise deposited metal patterns and thus requires surface protection. The impact of the temperature error is more pronounced for materials under test with low densities which thus produce smaller bandwidth and frequency shifts and undergo large temperature changes.

#### 2.4. Novel 'trough guide' resonator

In order to solve the described temperature problem and simultaneously arrive at a rugged design, a novel stray field resonator was devised (Knoechel *et al* 2003), built and tested. The construction is shown in figures 11(a)–(c). The resonator is completely manufactured from alumina ( $\text{Al}_2\text{O}_3$ ) in order to achieve the required abrasion protection directly. Figure 11(a) shows the top view. The resonator is implemented as a dielectrically filled 'trough guide', and consists of a cylindrical ring of a ceramic material metallized on its surface except at the top face of the ring cylinder, which is apparent as a bright circle. The  $\text{Al}_2\text{O}_3$  protection plate and possible glue layer are obsolete. There is no etched metal layer present on the upper face of the resonator. The metallized ring is soldered into a plate of stainless steel (or another metal). The inner area of the ring is also covered by a soldered metallic plate. Figure 11(b) shows a view of the lower side with two coaxial connectors for

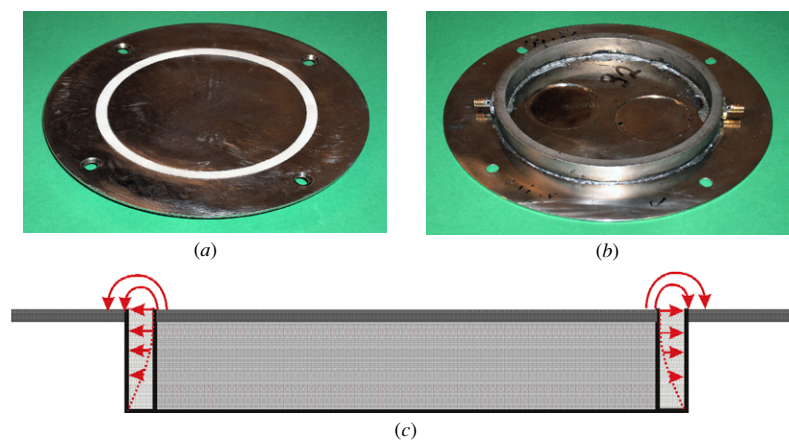


**Figure 11.** Construction of the 'trough guide' ring resonator. (a) Photograph of upper side, (b) lower side, (c) schematic drawing of cross section.

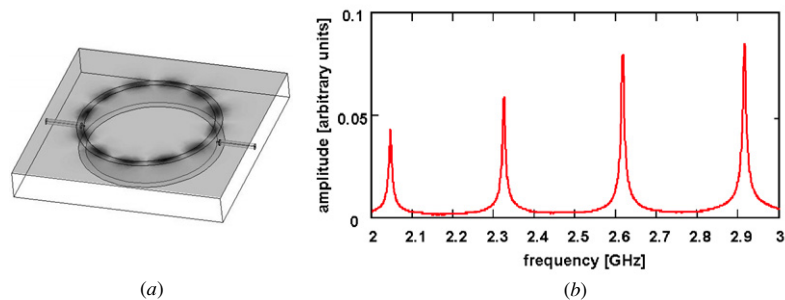


**Figure 12.** (a) Electrical field variation in the circumferential direction. Each dark-shaded area denotes the field strength distribution over half a wavelength. (b) Resonance spectrum in the frequency range between 2 and 3 GHz.

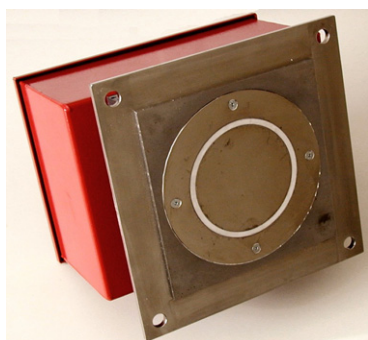


**Figure 13.** The new ring resonator mounted on a cabinet, together with the required electronic circuits.

coupling energy to the resonator. Resonances are excited if an integer number of full wavelengths fits along the circumference of the ring. Their electric fields are polarized tangentially to the upper open surface in the radial direction. The stray fields of the resonances extend into the outer space (figure 11(c)). The radial electrical field distributions vary as  $1/r$  but can be considered as virtually constant across the upper face of the ring. The field variation in the axial (height) direction is sinusoidal. The height of the ring amounts to a little bit more than a quarter wavelength in the dielectric.

The electrical field variation in the circumferential direction for one of the resonances is shown in figure 12(a). There are six full wavelengths appearing around the circumference in a sinusoidal distribution. Regions of high field intensity are represented by dark shades. The resonance spectrum is depicted in figure 12(b). It is quite similar to that of the microstrip sensor and each of the resonances can be used for measurement purposes. The new resonator exhibits a lower cut-off frequency, which is slightly above 1 GHz and can be adjusted mainly by changing the height of the ring. A photograph of the new resonator is shown in figure 13. In that picture, the ring is mounted on a cover plate of stainless steel. The required microwave and microprocessor electronics are situated in the box below the resonator to form a full moisture and density meter, suitable for operation in a harsh environment. The measured performance of this resonator is shown in figure 14. The change of the resonator bandwidth is plotted versus the change of the resonant frequency for the moisture values of 5.1% (lower bold curve) and 10.2% (upper bold curve). The density (mass) in the measurement volume is varied as denoted by the open circles. Each new

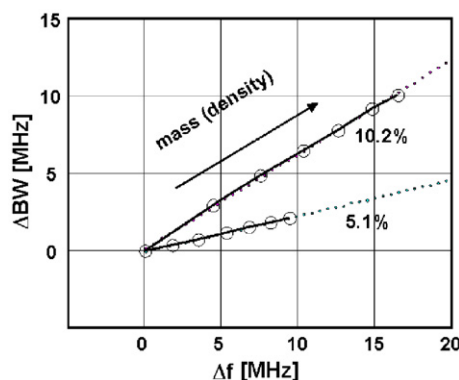


**Figure 14.** Performance when loaded with moist material.

circle means the additional deposition of the same amount of mass on the top of the resonator. As can be easily seen, the slope of the bold lines represents the moisture value, given by equation (2). The resonator can be calibrated by loading it with a single sample of a material with known moisture content, but preferably several different sample masses should be applied to improve the accuracy. In a similar way, a calibration for the density (mass) is possible by analysis of the distance in the direction of the circles on a straight line of constant moisture content.

Under constant environmental conditions, the sensibilities and accuracies for the moisture content or density measurements of the new and old resonator designs are exactly the same. This is a consequence of the measurement principle, which exploits differences of loaded and empty resonators. The stability of the resonator designs versus undesired external influences is thus most important.

### 2.5. Temperature characteristics of the ‘trough guide’ resonator

Six ‘trough guide’ resonators have been investigated over temperature in the same manner as already described for the microstrip resonators. The results are shown in figure 15. In comparison to the microstrip resonators, the resonant frequency variation over the observed temperature range of 20–50 °C increases from approximately 600 kHz (TMM10 in the specific assembly) to 4.5 MHz (Al<sub>2</sub>O<sub>3</sub>). This is due to the fact that for the new resonators the temperature coefficient of the permittivity of Al<sub>2</sub>O<sub>3</sub> ceramic is effective

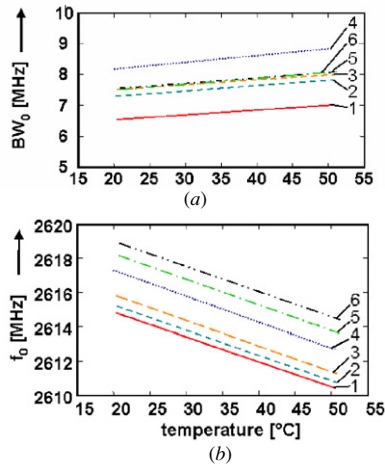


**Figure 15.** Temperature cycling of six different ‘trough guide’ resonators. Temperature cycling was the same as for microstrip resonators. (a) Temperature behaviour of bandwidth and (b) of resonant frequency. The numbers correspond to the respective resonators.

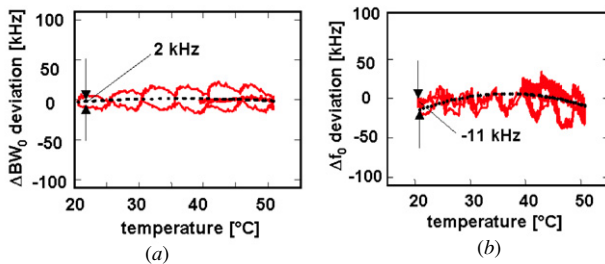


**Figure 16.** Frequency deviation from linear behaviour of (a) bandwidth and (b) resonant frequency versus temperature. The solid curves indicate the characteristics of one of the resonators, whereas the broken curves denote the average of the six investigated resonators.

for the determination of the resonant frequency, which is  $+199 \text{ ppm } ^\circ\text{C}^{-1}$ . The loss tangent of alumina is 0.0002, and thus by a factor 10 less than that of TMM10 (0.0023). This reflects the fact that TMM10, which has a temperature coefficient of the permittivity of  $-38 \text{ ppm } ^\circ\text{C}^{-1}$ , is a temperature-compensated dielectric composite, whereas alumina is a pure material. Temperature cycling shows that the resonant behaviour of alumina resonators depends on temperature in a highly linear fashion. Hysteresis effects obviously do not occur.

The advantageous temperature behaviour of the ‘trough guide’ resonators can clearly be seen from frequency deviations from the strictly linear characteristics, which are depicted in figures 16(a) and (b). As already explained for the microstrip resonators, temperature was changed in  $5 \text{ }^\circ\text{C}$  steps and then kept constant in order to allow the settling of thermal equilibrium. Figures 16(a) and (b) show solid lines, which describe the performance of one of the resonators, and broken lines, which depict the averages of the six resonators, respectively. There are upper and lower curve branches because of heating to  $50 \text{ }^\circ\text{C}$ , the down- and up-cycling of the temperature to  $20 \text{ }^\circ\text{C}$  and back to  $50 \text{ }^\circ\text{C}$  and the final process of slowdown cooling. The points where the branches meet

are those of approximate thermal equilibrium. In between, dynamic processes of heat propagation take place, which are not of interest for the present investigation.

The maximum deviations from the linear characteristics occur again at the temperature of  $20 \text{ }^\circ\text{C}$ . Here the deviation from linearity for the bandwidth is only  $d\Delta BW_0 = -2 \text{ kHz}$ , whereas for the resonance frequency, a linearity deviation of  $d\Delta f_0 = -11 \text{ kHz}$  is observed. The same test material as for the microstrip resonators is supposed to load the resonator: its moisture content is assumed to be  $\Psi = 10\%$  at a certain material density, and a bandwidth increase of  $\Delta BW = 500 \text{ kHz}$  and a frequency shift of  $\Delta f = 2500 \text{ kHz}$  take place when loading the resonator. Combining these values with the errors through linearity deviations now leads to a peak error of  $\Delta\Psi = 0.004\%$  in the measured moisture content. This extremely low value is caused by the fact that both relative errors ( $d\Delta BW_0/\Delta BW$  and  $d\Delta f_0/\Delta f$ ) are of roughly equal magnitude and nearly cancel each other! But even if they added, the error would be less than  $\Delta\Psi = 0.1\%$ . It is thus demonstrated that the new resonator offers the capability of keeping the temperature error at a negligible level under the assumption of linear temperature behaviour. The only preconditions which must be fulfilled with sufficient accuracy are

- homogeneous temperature of the resonator and
- determination of that temperature with sufficient accuracy.

The first condition requires a sufficiently slow temperature change and/or a suitable construction which assures good heat distribution. The second condition can be fulfilled by accurate placement of temperature sensors.

The ‘trough guide’ resonators are also superior to ceramic-filled plastic material (TMM10) microstrip resonators in other aspects. They can easily withstand elevated temperatures up to  $130 \text{ }^\circ\text{C}$  and more. This temperature stability can be attributed to the soldered in ceramic construction. In comparison, the ceramic-filled plastic material (TMM10) microstrip resonators can only be used up to approximately  $60\text{--}70 \text{ }^\circ\text{C}$ . Bending takes place due to unequal expansion coefficients of the ceramic-filled plastic material, the glue and the alumina cover sheet, combined with mechanical tensions in the various materials. When cycling the temperature, these tensions also have an adverse influence on the ageing behaviour of the whole assembly. The adhesive may become brittle after some time. The protective cover then detaches from the resonator, making the sensor defective.

### 3. Conclusions

Microwave stray field resonators for moisture content or density measurements can be manufactured from ceramic-filled plastic substrates with copper cladding. Various resonator patterns can be defined by etching. In practice such resonators require a cover for protection against abrasive forces, which is realized by gluing a thin sheet of alumina oxide onto the etched circuit. Such a multilayer circuit is prone to increased temperature sensitivity of the resonant frequency and resonator bandwidth including hysteretic behaviour, which can make the resonant properties unpredictable after temperature changes. The moisture content and density measurements

are deduced from the changes of resonance frequency and bandwidth with respect to the empty resonator. If the reference measurement on the empty resonator is made at an early stage, and the material measurement is carried out later after some cycling of the temperature, a precise measurement may become impossible with such equipment. In practice, the reference measurement of the empty resonator often cannot be repeated at a later time, because in a production process the resonator is permanently loaded by the material under test.

By taking advantage of a 'trough guide' ring resonator, measurement sensors are proposed and demonstrated in this paper which have the same measurement sensibility and accuracy with respect to moisture or density measurements but are by far superior to the conventional stray field resonators with multilayer construction concerning stability against undesired environmental disturbances. The new resonators are manufactured from alumina oxide ceramic rings. Their surface is metallized with the exception of the upper face, which is in contact with the material under test. The ceramic ring is soldered into a metallic surface. Thus it can also be implemented for areas where intrinsic safety is required. The ceramic resonator structure itself provides a rugged design

and excellent stability against abrasive forces. It also offers excellent temperature stability after applying a temperature measurement and assuming a linear temperature model. It is shown that the resulting temperature error in the moisture measurement can result in an error for the moisture value of well below 0.1%. Thus the influence of the resonator temperature on the accuracy is negligible in most practical cases.

## References

- Flemming M A and Plested G N 1988 Microwave probe comprising a resonant element *UK Patent Application* GB 2 202 947 A
- Herrmann R and Zaage S 2001 Microwave leakage field sensor for measuring moisture and/or density *US Patent* US 6,316,946 B2
- Knoechel R, Taute W and Doescher C 2003 Microwave stray field resonator *European Patent* EP 1 437 588 B1
- Meyer W and Schilz W M 1980 A microwave method for density independent determination of the moisture content of solids *J. Phys. D: Appl. Phys.* **13** 1823–30
- Rogers Corporation 2002 TMM temperature stable microwave materials as a replacement for alumina on space flight hardware *Datasheet TM 2.9.9* <http://www.rogerscorporation.com>